Published in final edited form as:
*J Biol Chem*. 2007 October 19; 282(42): 31085–31093.

# Nitro-fatty Acid Reaction with Glutathione and Cysteine:

## KINETIC ANALYSIS OF THIOL ALKYLATION BY A MICHAEL ADDITION REACTION*

**Laura M. S. Baker**‡, **Paul R. S. Baker**‡,[1], **Franca Golin-Bisello**‡, **Francisco J. Schopfer**‡,[2], **Mitchell Fink**§, **Steven R. Woodcock**‡,¶, **Bruce P. Branchaud**¶, **Rafael Radi**||,[3], and **Bruce A. Freeman**‡,[4]

‡ *Department of Pharmacology, University of Pittsburgh, Pittsburgh, Pennsylvania 15261*

§ *Department of Critical Care Medicine, University of Pittsburgh, Pittsburgh, Pennsylvania 15261*

¶ *Department of Chemistry, University of Oregon, Eugene, Oregon 97403*

|| *Departmento de Bioquímica, Facultad de Medicina, Universidad de la Republica, 11800 Montevideo, Uruguay*

## Abstract

Fatty acid nitration by nitric oxide-derived species yields electrophilic products that adduct protein thiols, inducing changes in protein function and distribution. Nitro-fatty acid adducts of protein and reduced glutathione (GSH) are detected in healthy human blood. Kinetic and mass spectrometric analyses reveal that nitroalkene derivatives of oleic acid (OA-$NO_2$) and linoleic acid ($LNO_2$) rapidly react with GSH and Cys via Michael addition reaction. Rates of OA-$NO_2$ and $LNO_2$ reaction with GSH, determined via stopped flow spectrophotometry, displayed second-order rate constants of 183 $M^{-1}s^{-1}$ and 355 $M^{-1}s^{-1}$, respectively, at pH 7.4 and 37 °C. These reaction rates are significantly greater than those for GSH reaction with hydrogen peroxide and non-nitrated electrophilic fatty acids including 8-*iso*-prostaglandin $A_2$ and 15-deoxy-$\Delta^{12,14}$-prostaglandin $J_2$. Increasing reaction pH from 7.4 to 8.9 enhanced apparent second-order rate constants for the thiol reaction with OA-$NO_2$ and $LNO_2$, showing dependence on the thiolate anion of GSH for reactivity. Rates of nitroalkene reaction with thiols decreased as the p$K_a$ of target thiols increased. Increasing concentrations of the detergent octyl-$\beta$-D-glucopyranoside decreased rates of nitroalkene reaction with GSH, indicating that the organization of nitro-fatty acids into micellar or membrane structures can limit Michael reactivity with more polar nucleophilic targets. In aggregate, these results reveal that the reversible adduction of thiols by nitro-fatty acids is a mechanism for reversible post-translational regulation of protein function by nitro-fatty acids.

The post-translational modification of proteins by electrophilic products of oxidative reactions has been viewed as a dosimeter of cytotoxicity (1). In the context of tissue inflammation and its resolution, reactions of redox-derived electrophiles are now also emerging as adaptive events induced by the modification of functionally significant thiols and other nucleophilic moieties of signaling proteins. Endogenous electrophiles include decomposition products of fatty acid hydroperoxides such as 4-hydroxynonenal (4-HNE)[5] and 4-*oxo*-2-nonenal (4-ONE), which form adducts with DNA bases and nucleophilic amino acids (2,3). Additionally, some

*This work was supported in part by National Institutes of Health Grants HL58115 and HL64937 (to B. A. F.) and AHA Grant 0450118Z (to B. P. B.), and a Department of Education GAANN (Graduate Assistance in Areas of National Need) award (to S. R. W.).

4 To whom correspondence should be addressed: Dept. of Pharmacology, Thomas E. Starzl Biomedical Science Tower, 200 Lothrop St, University of Pittsburgh, Pittsburgh, PA 15213. Tel.: 412-648-9319; Fax: 412-648-2229; E-mail: freerad@pitt.edu.

[1]Supported by the American Diabetes Association.
[2]Supported by a Beginning Grant In-Aid from the AHA.
[3]Supported by the Howard Hughes Medical Institute (U. S. A.) and International Centre of Genetic Engineering and Biotechnology (Italy).

isoprostanes and cyclopentenone prostaglandins, including prostaglandins $J_2$ and $A_2$ and their metabolites, display anti-inflammatory, anti-viral, and cytoprotective actions that are directly attributable to the electrophilic nature of their $\alpha,\beta$-unsaturated carbonyl group (4).

Electrophile-induced signal transduction occurs via a number of thiol-dependent mechanisms. The increased expression of Phase II enzymes and oxidant detoxification mechanisms occur via activation of a cis-acting electrophile-responsive element (EpRE, also known as the antioxidant responsive element, ARE) (5,6). Inhibition of nuclear translocation and DNA binding of the transcription factor Nrf2, a critical regulator of EpRE-dependent transcription, is reversed upon electrophile reaction with the thiol-containing repressor protein, Keap1 (kelch-like ECH-associated protein-1). Keap1 thiol reaction with diverse electrophiles alters association with a scaffold protein Cullen3 to release Nrf2 for nuclear translocation and promotion of expression of Phase II genes (7–9), including GSH biosynthetic enzymes (10) and heme oxygenase 1 (HO-1) (11). Gene expression of pro-inflammatory cytokines is also inhibited by electrophiles. For example, electrophilic alkylation of the pro-inflammatory transcription factor, nuclear factor-$\kappa$B (NF-$\kappa$B) modifies critical thiols in the p65 and p50 subunits, in turn suppressing DNA binding and NF-$\kappa$B target gene activation (12–16). Fatty acid-derived electrophiles also serve as ligands for receptors activated by the modulation of a critical Cys; for example, 15-deoxy-$\Delta^{12,14}$-$PGJ_2$ (15dPG$J_2$) binds to peroxisome proliferator-activated receptor-$\gamma$ (PPAR$\gamma$), increasing transcription of PPAR response element-regulated genes (17–19). Of note, electrophiles also modulate the activities of nervous system targets such as synaptic proteins (20) and the excitatory ion channel, TRPA1 (21,22) by alkylating critical thiols. This mode of signal transduction is distinct from more traditional non-covalent ligand-receptor interactions that elicit responses by inducing conformational changes.

Nitric oxide ($^{\bullet}$NO)-derived reactive species both oxidize and nitrate unsaturated fatty acids, yielding an array of hydroxy, hydroperoxy, nitro, and nitrohydroxy derivatives that transduce host defense and cell signaling actions of $^{\bullet}$NO (23–29). Nitro derivatives of linoleic acid ($LNO_2$) and oleic acid (OA-$NO_2$) have been detected clinically and prepared synthetically, with their cell signaling actions currently being defined. Present insight indicates that nitroalkenes, via cGMP-independent mechanisms, mediate metabolic and anti-inflammatory responses as a consequence of their electrophilic reactivity, a potent ability to regulate gene expression and PPAR activation (25,26,30,31). These beneficial adaptive responses are distinct from the pathogenic actions typically associated with membrane and lipoprotein-derived hydroxy-, carbonyl-, and hydroperoxy-containing unsaturated fatty acid derivatives (1). Of exception to this latter precept is growing evidence that adaptive anti-inflammatory signaling mediators are also formed by autocatalytic and enzymatic oxidation of fatty acids. These mediators include the resolvin class of eicosanoid oxidation products (32,33), electrophilic cyclopentenone $A_2$ and $J_2$ isoprostanes (4) and other omega-3 fatty acid oxidation products (34).

Recently, it was reported that nitrated fatty acid derivatives potently inhibit cytokine and inducible nitric oxide synthase expression in LPS and interferon-$\gamma$-stimulated monocytes by alkylating critical thiols in the DNA binding region of the NF-$\kappa$B p65 subunit (26). In support of the concept that fatty acid nitroalkene derivatives manifest cell signaling actions via an electrophilic reactivity, proteomic analysis reveals alkylation of nucleophilic amino acids such

[5]The abbreviations used are: 4-HNE, 4-hydroxynonenal; OA-$NO_2$, nitrated oleic acid; $LNO_2$, nitrated linoleic acid; $^{\bullet}$NO, nitric oxide; GSH, reduced glutathione; ONE, 4-oxononenal; $ONOO^-$, peroxynitrite; $H_2O_2$, hydrogen peroxide; isoP$GA_2$, 8-*iso*-prostaglandin $A_2$; 15dP$GJ_2$, 15-deoxy-$\Delta^{12,14}$-prostaglandin $J_2$; $S^-$, thiolate; PPAR, peroxisome proliferator-activated receptor; GS-$LNO_2$, nitroalkylated linoleic acid; GS-OA-$NO_2$, nitroalkylated oleic acid; HPLC ESI MS/MS, high performance liquid chromatography electrospray ionization triple quadrupole mass spectrometry; MRM, multiple reaction monitoring; CID, collision-induced dissociation; TIC, total ion count; and *m*/*z*, mass to charge ratio; OG, octyl-$\beta$-D-glucopyranoside.

as Cys and His (35), not unlike the protein adduction reactions mediated by HNE, ONE, 15dPGJ$_2$, and 8-*iso*-prostaglandin A$_2$ (isoPGA$_2$) (3).

Because the nitro group is one of the strongest electron-withdrawing functional groups known (36,37), the conjugation of the nitro group with an alkene will confer exceptionally electrophilic properties and support robust Michael addition reactions by nitroalkenes. In biological milieu, such Michael reactions occur as a conjugate addition of nucleophilic centers to the electrophilic carbon $\beta$-to the nitro-bonded carbon in the nitroalkene (Fig. 1) (35). Evidence of GSH nitroalkylation *in vitro* and *in vivo* was obtained from electrospray ionization (ESI)-ion trap mass spectrometric analysis of healthy human red blood cells (35). GSH conjugates with xenobiotics and cellular electrophiles (35,38,39) and reacts with nitrated fatty acids to form, GS-OA-NO$_2$ and GS-LNO$_2$ derivatives detectible at 3.3 and 1.3 nM, respectively. Additionally, GS-LNO$_2$ was detected in cultured MCF7/WT cells, with the *in vivo* levels of adducts dependent on expression levels of MRP1, an efflux transporter of GSH conjugates (44). Collision-induced dissociation (CID) of nitroalkylated GSH and structural analysis by MS/MS/MS affirm that nitroalkenes are bonded to nucleophilic Cys residues (35). Additionally, protein Cys residues are readily adducted by lipid-derived electrophiles (35, 40). Protein conjugates with nitroalkenes have also been detected in healthy human red blood cells, with specific sites of glyceraldehyde-3-phosphate dehydrogenase (GAPDH) nitroalkylation occurring *in vitro* and *in vivo* mapped via matrix-assisted laser desorption and ionization time of flight mass spectrometry (MALDI-TOF MS). Importantly, protein nitroalkylation reactions are reversible by physiologic concentrations of GSH (35).

Herein, we report the reaction kinetics of nitroalkenes with GSH and Cys, and compare the derived rate constants with reaction rates of other biologically relevant electrophiles. Determination of second-order rate constants provides a concentration-independent proportionality factor for the reaction rate and allows for comparison to other GSH-electrophile reactions carried out under disparate conditions. We observed that fatty acid nitroalkene derivatives react with GSH and Cys via a Michael addition mechanism at bimolecular rate constants exceeding most fatty acid-derived electrophiles.

## EXPERIMENTAL PROCEDURES

### Materials

Mixed regioisomers of OA-NO$_2$ and LNO$_2$ (9- and 10-nitro-9-*cis*-octadecenoic acid and 9-, 10-, 12-, and 13-nitro-9,12-*cis*-octadecadienoic acid) were synthesized as prepared previously (24,27). The specific regioisomer 9-nitro-9-*cis*-octadecenoic acid ($C^9$-OA-NO$_2$) was synthesized as described (41). Linoleic and oleic acids were from Nu-Check Prep (Elysian, MN). 15dPGJ$_2$ and isoPGA$_2$ were from Cayman Chemical (Ann Arbor, MI). Methyl-2-acetamidoacrylate (M2AA) and ethyl pyruvate (EP) were gifts from Mitchell Fink. Diethylenetriamine pentaacetate (DTPA), $H_2O_2$, L-glutathione, L-cysteine, dihydroxy lipoic acid (DHLA), DL-homocysteine, *N*-acetyl-cysteine, DL-penicillamine, L-cysteine methyl ester hydrochloride, 5,5′-dithiobis(2-nitrobenzoic acid) (DTNB), catalase (from bovine liver), dimethyl sulfoxide (Me$_2$SO), and *N*-octyl-$\beta$-D-glucopyranoside were from Sigma-Aldrich. Potassium phosphate dibasic and monobasic and Tris buffer components were from Fisher Scientific.

### Spectrophotometric Characterization of Nitro-fatty Acid Reactions

OA-NO$_2$ and LNO$_2$ stock solution concentrations were analyzed in phosphate buffer (100 mM, pH 7.4) containing 100 $\mu$M DTPA, an iron chelator, at 270 nm using a UV-VIS spectrophotometer (Shimadzu, Japan). The extinction coefficients ($\varepsilon$) used to calculate the concentrations of OA-NO$_2$ and LNO$_2$ were 8220 $M^{-1}cm^{-1}$ and 8650 $M^{-1}cm^{-1}$, respectively

(27). Reactions of nitro-fatty acids with GSH were characterized spectrophotometrically using an Agilent 8453 diode array spectrophotometer (Santa Clara, CA) over a range of 200–400 nm at 20 °C, pH 7.4.

### Determination of Second-order Rate Constants

Reactions were conducted on an Applied Photophysics SX-20 stopped-flow spectrophotometer (Surrey, UK) at 37 °C, and the decrease in $NO_2$-fatty acid absorbance at 285 nm was monitored over time. Reactions were initiated by mixing the $NO_2$-fatty acid (20 $\mu$M, pre-diluted in MeOH) with increasing concentrations of GSH (or other thiol-containing compounds, 0–2 mM) in 100 mM potassium phosphate buffer, pH 7.4 containing 100 $\mu$M DTPA. In all experiments, indicated reactant concentrations are given as final concentrations achieved after mixing. Apparent pseudo-first-order rate constants were obtained by fitting the reaction progression curves from 0.2–10 s with the single exponential function with a floating end point from the curve-fitting algorithm embedded in the Pro-Data software (Applied Photophysics) and plotted against [GSH]. The slope of the line resulting from a linear regression curve fit of the data is equal to the apparent second-order rate constant, $k_{app}$. Total time for reactions was 10 s. All second-order rate constant data obtained are expressed as mean ± S.D. and are from three or more independent experiments.

### Time-dependent Spectral Studies

To obtain spectral scans over shorter times (0–2 s), the spectrakinetic setting was used on the stopped flow. Volumes of 5 ml were prepared, and the instrument was set to record reactions for 2 s at each wavelength between 300 and 245 nm. Multi-wavelength kinetic data were analyzed using the Pro-Kineticist software package (Applied Photophysics).

### Thiol Oxidation by $H_2O_2$ and Electrophilic Lipids

The slower rates of GSH oxidation and alkylation by $H_2O_2$ and electrophilic fatty acid derivatives were determined by removing aliquots from a reaction mixture containing non-saturating amounts of GSH (0.388 mM) and excess oxidant/electrophile (1.3 mM) and then monitoring each aliquot for sulfhydryl content as described (42). Briefly, samples were incubated at 37 °C with shaking, and aliquots were removed every 60 s. When $H_2O_2$ was added to the GSH reaction mixture, remaining $H_2O_2$ was removed from aliquot by addition of 10 units/ml catalase prior to sulfhydryl analysis at 412 nm using DTNB ($\varepsilon = 1.415 \times 10^4$ $M^{-1}cm^{-1}$). For the addition of electrophile to GSH, reactions were stopped with 5× DTNB and immediately diluted into 50 mM Tris, pH 8.0 and analyzed for sulfhydryl content. The equation used to describe the rate of reaction between $H_2O_2$ and electrophiles with sulfhydryls is shown in Equation 1,

$$1 \Big/ (nH_o - S_o) \ln [(S_o(H_o - S)) \Big/ (H_o(S_o - nS))] = k'_{HS} t \qquad \text{(Eq. 1)}$$

where $H_o$ and $S_o$ represent the initial concentrations of reactant and sulfhydryl, respectively, S is the sulfhydryl consumed after time *t*, *n* represents mol sulfhydryl oxidized per mol peroxide and $k'_{HS}$ is the apparent second-order rate constant of the reaction. The value of *n* was assumed to be two for the reaction between GSH and $H_2O_2$, and one for the reaction of GSH with the electrophile (*e.g.* the formation of the GS-lipid conjugate) (42).

# RESULTS

## Spectrophotometric Characterization of Nitro-fatty Acid Reactions with GSH

Fatty acid nitroalkene derivatives display distinctive absorbance spectra compared with native fatty acids (Fig. 2*A*). A characteristic spectrum of $LNO_2$ in aqueous buffer yields an absorbance maximum at 270 nm because of olefin conjugation with the nitro group (27), while linoleic acid (LA) does not display absorbance outside the far UV region. Upon the addition of GSH, the absorbance maximum of $LNO_2$ was blue-shifted, and as the reaction progressed, there was a loss of absorbance at 270 nm and a gain of absorbance at 250 nm for both $LNO_2$ (Fig. 2*A*) and OA-$NO_2$ (Fig. 2*B*) GSH adducts. When comparing the absorbance spectra of thiol-adducted nitroalkenes (GS-$LNO_2$ and GS-OA-$NO_2$) with free nitrated fatty acids, there is minimal overlapping absorbance between the spectra of adducted and non-adducted at wavelengths greater than 285 nm. Subsequent studies monitored the decay in nitroalkene absorbance during reaction with GSH at 285 nm, where absorbance from the formation of GS-$LNO_2$ or GS-OA-$NO_2$ was decreased. It is assumed that the decay of OA-$NO_2$ absorbance occurs upon thiol adduction. Spectrakinetic scans show that an isosbestic point for the conversion OA-$NO_2$ to GS-OA-$NO_2$ did not occur until 0.2 s (data not shown). Multiple isosbestic points indicating intermediates were not detected before 0.2 s (not shown).

## Kinetic Analysis of Nitro-fatty Acid Reaction with GSH

To study the rate of nitroalkene reaction with various thiol compounds, an integral rate method under pseudo-first-order conditions was used. OA-$NO_2$ binds to the Cys of GSH with a negligible reverse reaction when no other thiols are present, according to Equation 2,

$$\mathrm{OA-NO_2 + GSH \xrightarrow{k} GS-OA-NO_2} \quad \text{(Eq. 2)}$$

where $k$ = second order rate constant. In the presence of excess GSH, OA-$NO_2$ decomposition follows an exponential function *versus* time (Fig. 3*A*), suggesting that the reaction is first order with respect to the nitroalkene concentration. Changes in [OA-$NO_2$] over time are expressed as Equation 3,

$$-\mathrm{d[OA-NO_2]}\Big/\mathrm{d}t = k[\mathrm{OA-NO_2}][\mathrm{GSH}] = k'[\mathrm{OA-NO_2}]\mathrm{d}t \quad \text{(Eq. 3)}$$

where $k'$ (or $k_{obs}$) is the pseudo-first-order rate constant, $k$[GSH]. Integration of Equation 3 gives Equation 4.

$$\ln\left([\mathrm{OA-NO_2}]\Big/[\mathrm{OA-NO_2}]_o\right) = k't \quad \text{(Eq. 4)}$$

Taking the anti-log of Equation 4 gives an exponential function shown in Equation 5,

$$[\mathrm{OA-NO_2}] = [\mathrm{OA-NO_2}]_o e^{-k't} \quad \text{(Eq. 5)}$$

to which all reaction progressions were fit to obtain $k'$. When $k'$ was plotted as a function of [GSH], a linear response was obtained (Fig. 3*B*), confirming that the reaction is first order in GSH. The slope of the secondary plot yielded the apparent second-order rate constant ($k_{obs}$ = $k$[GSH]) for the reaction of GSH with a particular nitroalkene concentration (Table 1).

Biological and chemical nitration of unsaturated fatty acids yields an array of regioisomers (28,43,44). There was no significant difference in apparent second-order rate constants for the reaction of GSH with mixed regioisomers of OA-$NO_2$ and the specific regioisomer $C^9$-OA-

$NO_2$ (Table 1), while the rate constant for $LNO_2$ reaction with GSH was 1.9 times faster than the mixed regioisomers of OA-$NO_2$ and $C^9$-OA-$NO_2$. The rate constants for Cys reaction with both nitroalkenes were ~1.5 times faster than for those with GSH.

## Comparison of Second-order Rate Constants

Determination of rate constants for thiol-nitroalkene reactions provides a proportionality constant which allows for reactions to be compared in a manner independent of the concentration of the reactants. The apparent second-order rate constants determined herein show that reactions occur at biologically-relevant rates (Table 1). The rates of GSH reaction with OA-$NO_2$ and $LNO_2$ were 140–267 times faster than with 4-HNE (1.33 $M^{-1}s^{-1}$) (45), similar to GSH reaction with 4-oxononenal (145 $M^{-1}s^{-1}$) (39), less than for the GSH reaction with other highly thiol-reactive biological oxidants such as $ONOO^-$, carbonate radical and nitrogen dioxide (46) (Table 2) and similar to a previous report (44). While some data were obtained from reports where concentrations of reactants may have differed from herein, rate constant comparisons still allow for nitroalkene reactivity to be examined in the context of other biological oxidants and electrophiles.

The reaction of $H_2O_2$ with GSH was evaluated at 37 °C and pH 7.4 using an indirect method in which the reaction was assessed by quantifying over time the residual GSH thiol content after oxidant exposure, yielding an apparent second-order rate constant of 2.6 $M^{-1}s^{-1}$ (Table 2). This value is 1.8 times less than for a previously-reported rate of oxidation of Cys by $H_2O_2$ (42), 4.69 $M^{-1}s^{-1}$, and is in accordance with the ~1.5 times difference between the GSH and Cys apparent second-order rate constants for reaction with nitroalkenes (Table 1).

Two eicosanoid derivatives, isoP$GA_2$ and 15d$PGJ_2$, have been reported to form adducts with GSH, albeit in the presence of the catalyst glutathione-S-transferase (47,48). To compare non-enzymatically-catalyzed GSH reactivity of nitroalkenes with these lipids, a similar indirect method was used, wherein remaining DTNB-titratable GSH was quantified over time (as above). The reactivity of both eicosanoids with GSH was 3.7 times less than the rate of $H_2O_2$ reaction with GSH (Table 2) and ~260 to 500 times less than for OA-$NO_2$ and $LNO_2$ reaction with GSH, respectively (Table 2).

When nitroalkene reactivity was evaluated by directly comparing the decrease in GSH thiolate availability over time using the same concentrations of products and reaction conditions as for the eicosanoids, a rapid loss of [SH] was observed for OA-$NO_2$ reaction with GSH. This was not observed for the eicosanoids, highlighting significant differences in electrophilic reactivity (Fig. 4*A*). Nearly all GSH thiols were consumed within 60 s upon reaction with OA-$NO_2$, with minimal or no consumption of [SH] by eicosanoid derivatives and vehicle control at this time point. This indicates that fatty acid nitroalkene derivatives are significantly more reactive with GSH than electrophilic fatty acid cyclopentenone derivatives.

Another anti-inflammatory electrophile that can form thiol adducts is ethyl pyruvate (EP). This species is derived from pyruvic acid and is effective as a therapeutic agent in sepsis and hemorrhagic shock (49,50). Comparison of the reactivity of GSH with nitroalkenes, EP and its derivative methyl-2-acetamidoacrylate (M2AA), again revealed that the OA-$NO_2$ reaction resulted in rapid loss of [SH] (Fig. 4*B*) with little reduced GSH remaining after 60 s. In this same time frame, residual thiol concentration in solutions containing EP and M2AA were nearly equivalent to that of the $Me_2SO$ vehicle. M2AA exhibits anti-inflammatory properties that exceed those of EP (51); consistent with this, it was observed that M2AA displays a greater apparent second-order rate constant for reaction with GSH (0.4 $M^{-1}s^{-1}$) than EP (0.05 $M^{-1}s^{-1}$) (Fig. 4*B*).

### The Effects of pH on Nitroalkene Reactivity

The thiolate anion is a far more potent nucleophile than other available biological nucleophiles such as amines, imidazoles, or protonated thiols (52,53). This reactivity of thiolate anions with nitroalkenes has been shown to be favored over amine addition at comparable p$K_a$ (54). The Michael reaction between nitroalkenes and GSH presupposes that the thiolate anion of GSH ($GS^-$) attacks the olefinic carbon $\beta$ to the nitro group of the fatty acid. Therefore, an elevated pH should increase the rate of GSH reaction with nitroalkenes, given that relative concentrations of $GS^-$ will be greater at higher pH values (p$K_a$ of GSH thiol = 8.8). Determination of the pH dependence of second-order rate constants for GSH reaction with nitroalkenes revealed an exponential acceleration of reaction rate until pH 8.9 (Fig. 5). The decrease in rate at pH values below 7.4 is not only due to low $S^-$ availability but also a possible consequence of accelerated Nef-like nitroalkene decay reactions (52) and decreased solubility of nitroalkene fatty acid derivatives in acidic solutions (not shown). $LNO_2$ displays a greater relative reactivity with GSH compared with OA-$NO_2$ at all pH values tested, although the pH profile for $LNO_2$ reaction with GSH is the same as for OA-$NO_2$ (Fig. 5).

### The Influence of Thiol p$K_a$ on Nitroalkene Reactivity

Because the apparent second-order rate constants for the reaction of nitroalkenes with Cys were greater than for GSH (Table 1), the reactivity of nitroalkenes with low molecular weight thiols having different thiol p$K_a$ values was examined. There was a general correlation between the thiol reaction rates of OA-$NO_2$ and thiol p$K_a$, wherein with decreasing thiol p$K_a$ and thiolate availability, there is a decreased apparent second-order rate constant at pH 7.4 (Table 3). For example, OA-$NO_2$ reaction with homocysteine (thiol p$K_a$ = 8.9) gave an apparent second-order rate constant 1.8 times less than for OA-$NO_2$ reaction with GSH, which displays a p$K_{(SH)}$ of only 0.1 pH unit less than for homocysteine. Accordingly, the reaction of OA-$NO_2$ with cysteine methyl ester (p$K_a$ = 6.7) displayed an apparent second-order rate constant 1.7 times greater than that for the reaction of Cys with OA-$NO_2$. For dihydrolipoic acid (DHLA), assuming that both thiols react with OA-$NO_2$ at equal rates, the non-transformed value of 26.6 $M^{-1}s^{-1}$ obtained by fitting the reaction progressions with the exponential rate function, would be 13.3 $M^{-1}s^{-1}$. Given that DHLA has a very high thiol p$K_a$, a low apparent second-order rate constant for nitroalkene was expected and observed.

### Inhibition of GSH Adduction by Detergent

To evaluate the effects of micellar organization on nitroalkene availability for GSH adduction reactions, the nitroalkene reaction with GSH was studied over a range of octylglucoside (OG) concentrations that encompass the critical micellar concentration (CMC, 3.5 mg/ml). For concentrations of OG below the CMC, rates of thiol-nitroalkene reaction increased (Fig. 6), suggesting that low detergent concentrations may promote nitroalkene solubility. As the CMC of OG is approached, rates of OA-$NO_2$ and $LNO_2$ reaction with GSH significantly decreased. At high OG concentrations, the lipid absorbance prior to the addition of GSH was not shifted and was comparable to lipid absorbance at low OG concentrations, indicating that OG additions did not interfere with the ability to follow the nitroalkene reaction spectrophotometrically.

## DISCUSSION

In 1988 Talalay *et al.* (5) presciently noted that a common feature of anti-carcinogenic Phase II enzyme inducers was their reactivity as Michael reaction acceptors. These inducing agents were characterized by olefinic bonds rendered electrophilic by conjugation with electron-withdrawing substituents, with their potency as Phase II inducers paralleling their efficiency in Michael reactions. Of note, a nitroalkene derivative (1-nitro-1-cyclohexene) was the most potent inducer of cellular quinone reductase activity reported in this early example of electrophile signaling.

There is now an expanding appreciation of the pluripotent adaptive cell signaling actions by electrophilic products of oxidative inflammatory reactions. These products include electrophilic cyclopentenones ($PGJ_2$, $A_2/J_2$ isoprostanes), 4-HNE and 4-ONE and other less characterized fatty acid oxidation products. These species all have a capacity to adduct nucleophilic residues of key regulatory mediators of cell signaling, including I$\kappa$B kinase, NF-$\kappa$B p50 and p65 subunits and Keap1 (9,12).

Recently, nitro derivatives of fatty acids have been identified as a class of endogenous cell signaling mediators that (*a*) serve as potent PPAR ligands (24,27), (*b*) release $^{\bullet}NO$ via a Nef-like decay reaction (55,56), (*c*) induce heme oxygenase-1 and endothelial nitric oxide synthase expression (30,31), (*d*) inhibit DNA binding of the p65 subunit of NF$\kappa$B and expression of downstream pro-inflammatory genes (26), and (*e*) undergo thiol-reversible Michael addition reactions with nucleophilic Cys and His residues (35). This latter electrophilic reactivity accounts for many of the aforementioned signaling actions of nitroalkenes and was the basis for the present study.

Kinetic characterization of the reaction of nitroalkenes with GSH capitalized on the absorbance characteristics of nitroalkenes and their reaction products. A rapid decrease in the spectral absorbance at 270 nm $LNO_2$ and OA-$NO_2$ occurs upon conjugation with thiols (Figs. 2 and 3). This allows for kinetic data to be gleaned from exponential decay curves, which represent 1) a loss of absorbance of free, solubilized nitroalkene, 2) rearrangement of the nitro-group electron conjugation to yield a new absorbance maximum, and 3) nitroalkene adduction to thiols. Using this strategy, stopped flow spectroscopic measurement and kinetic analysis revealed there was a greater rate constant for $LNO_2$ reaction with GSH than for OA-$NO_2$ (Table 1). The specific site of fatty acid nitration (*e.g.* the $C^9$-$NO_2$ or $C^{10}$-$NO_2$ of OA-$NO_2$) was not critical in determining rates of reaction with GSH, as evidenced by the similar reaction rate for the $C^9$ regioisomer of OA-$NO_2$ compared with the mixed regioisomer preparation (Table 1). Because of structural differences between OA-$NO_2$ and $LNO_2$, kinetic analyses of GSH reactions may not precisely reflect relative rates of OA-$NO_2$ and $LNO_2$ reaction with proteins. In this instance, steric restrictions dictated by Cys and His microenvironments (*i.e.* solvent-exposed *versus* more sterically restricted regions) may also add to the differential intrinsic reactivities of various fatty acid nitroalkene derivatives. The diverse reactivity of thiols suggests that multiple factors can also influence nucleophile reactivity and availability, including structural differences in nitrated lipids, $pK_{(SH)}$, nucleophilicity, solubility, intramolecular hydrogen-bonding, and steric restriction.

Second-order rate constants for nitroalkene-thiol reaction are equivalent to, or significantly greater than, those for other major electrophilic fatty acid oxidation products and biological oxidants (Table 2). Previous work has shown that GSH reacts with $PGJ_2$, $PGA_2$, ONE, and HNE to form thiol conjugates that in turn can mitigate the cell signaling actions of these species. In contrast with nitroalkenes, thiol adduction by these species is irreversible, thus limiting a dynamic role in mediating cell signaling. Additionally, the role of the above lipids in cell signaling is further muted by the fact that $PGJ_2$ and $PGA_2$ require the presence of GSH-transferase (GST) for adduction to GSH. In contrast, nitro-fatty acids can react with thiols at a high rate in the absence of GSTs, highlighting their increased ability to react with *in vivo* thiol-containing targets, where GST reactivity would not play a role in conjugation.

Because the thiolate anion is the most potent nucleophilic center in Michael reactions of thiols, the influence of pH on GSH reactivity with nitroalkenes was determined. The apparent second-order rate constant for the reaction of OA-$NO_2$ and $LNO_2$ with GSH increased as the pH approached the $pK_a$ of the GSH thiol (Fig. 4), with reaction rates relatively constant at pH > 8.9. At pH values lower than 7.2, there was minimal reactivity (data not shown) due to the protonation of the carboxylic acid group of the nitrated fatty acid, which decreased its solubility.

Nitroalkenes dispersed in aqueous milieu or polar solvents at low pH values are turbid, likely reflecting micellar distribution, which would sequester the lipid from reaction with more polar thiolate anions.

The apparent second-order rate constant for nitroalkene reaction with GSH was less than that determined for Cys (Table 1). The study of thiol p$K_a$ on nitroalkene reactivity revealed that, except for an anomalous rate of reaction with penicillamine (a sterically hindered thiol), an inverse relationship between thiol p$K_a$ and the value of the apparent second-order rate constant was observed (Table 3). The promotion of nitroalkylation by alkaline pH and low thiol p$K_a$ values is consistent with both the proposed Michael addition mechanism and the reaction of $ONOO^-$ with thiols of incrementing p$K_a$ values (46). It is also possible that the rate constants of nitroalkenes with fast reacting thiols (*e.g.* the catalytic thiol of peroxiredoxins) may be much faster, as observed for the reaction of $ONOO^-$ with tryparedoxin peroxidase (57).

Overall, most thiols and most nitroalkenes, regardless of their specific structures and chemical micro-environments, will be highly reactive with each other. Nitro-fatty acid partitioning into non-ionic detergent micelles and phospholipid liposomes will limit Nef-like reactions that in turn yield $^{\bullet}NO$, supporting the observation that nitroalkenes are stabilized by hydrophobic environments (55). Similarly, the reaction of GSH with OA-$NO_2$ and $LNO_2$ was inhibited by the micellar stabilization that occurs upon reaching the CMC of the non-ionic detergent, with a decrease in the $k_{obs}$ for GSH reaction observed for both OA-$NO_2$ and $LNO_2$ (Fig. 6). This suggests that when the electrophilic carbon $\beta$ to the nitro group is sequestered in hydrophobic environments, nitroalkenes become less accessible to nuceophilic attack by thiolate anions. Moreover, this implies that esterified nitroalkene derivatives may remain sequestered from many nucleophilic targets until periods of oxidative stress or inflammation promote de-esterification via phospholipase activation or upon disruption of membrane integrity. Thus, membrane bilayers and lipoproteins may act as a reservoir of nitroalkenes that can be released in a regulated manner.

Nitroalkene-induced post-translational modification of proteins affects both biomolecule function and anatomic distribution. Nitroalkylation of proteins promotes membrane association and influences the function of proteins having Cys and His residues critical for structure or catalysis (35). The nitroalkylation of protein thiols is GSH-reversible, yielding a GS-nitro-fatty acid exchange reaction product detectable in healthy human blood (35) and cell culture systems (44). The extracellular transport of GS-nitroalkene conjugation products can be mediated by the multi-drug resistance protein-1, a reaction that would be expected to mitigate cell signaling actions of nitroalkenes (44). Finally, nitroalkenes may facilitate *S*-glutathiolation of protein thiols in the course of exchange reactions, thus further influencing the regulation of structural, transport and catalytic protein function (58,59) in Equation 6.

$$PSH + GS - OA - NO_2 \rightarrow PSSG + OA - NO_2 \qquad \text{(Eq. 6)}$$

Protein *S*-glutathiolation is a functionally significant post-translational modification that is enhanced by oxidative stress and also serves as a mechanism to preserve GSH and protect protein thiols from oxidation to less reversible sulfenic and sulfonic acid derivatives (60). The nitroalkylation of GSH may thus predispose glutathionylation reactions, thereby expanding the spectrum of potential nitroalkene signaling actions.

The relatively rapid kinetics of nitroalkene-thiol reactions, compared with other biological electrophiles, requires additional study to understand the impact of nitroalkenes as signaling mediators. For example, nitroalkenes may preferentially react with target molecules in close proximity to sites of fatty acid nitration, thus possibly diminishing reaction with more remote cellular targets. Greater relative reaction rates with GSH may also promote extracellular efflux

of nitroalkenes by the multi-drug resistance protein or other GSH adduct transporters. Future analysis will reveal if this export mechanism also facilitates vascular or lymphatic transport of nitroalkenes to remote organs. The use of biochemical and cellular models will also reveal the influence of GSH transferases on the kinetics of *in vivo* nitroalkene adduction and trafficking.

An important, unresolved issue regarding the clinical potential of electrophiles as adaptive inflammatory mediators is the influence of their intrinsic reactivities on pharmacokinetics and biodistribution. For example, the electrophilic $\alpha,\beta$-unsaturated ketone moiety of 15d-$PGJ_2$, other prostaglandins and isoprostanes promotes an adduction with target molecules that is resistant to reversal by biological reductants. This in part accounts for the pM to low nM concentrations typically observed for non-adducted electrophilic lipids. Until quantitative proteomic strategies are developed that support the detection and quantitation of adducted electrophilic lipids, cogent estimates of their bioavailability and signaling actions in biologic systems will be lacking.

In summary, fatty acid nitration reactions yield potent anti-inflammatory products that link the metabolic and immuno-competent state of the host via specific post-translational protein modification reactions that transduce cell signaling events (26,31,44,61). Nitrated fatty acid species thus merge aspects of redox, nitric oxide and fatty acid signaling pathways in the form of a class of pluripotent adaptive signaling mediators. The kinetically favorable and reversible reaction of nitroalkenes with thiols is central in the post-translational protein modifications that underlie their signaling actions.

**Acknowledgements**

We thank Carlos Batthyany, M.D., Ph.D. for helpful conceptual guidance and Elizabeth J. Meade for technical assistance.

## References

1. Marnett LJ, Riggins JN, West JD. J Clin Investig 2003;111:583–593. [PubMed: 12618510]
2. Lee SH, Williams MV, Dubois RN, Blair IA. J Biol Chem 2005;280:28337–28346. [PubMed: 15964853]
3. Sayre LM, Lin D, Yuan Q, Zhu X, Tang X. Drug Metab Rev 2006;38:651–675. [PubMed: 17145694]
4. Straus DS, Glass CK. Med Res Rev 2001;21:185–210. [PubMed: 11301410]
5. Talalay P, De Long MJ, Prochaska HJ. Proc Natl Acad Sci U S A 1988;85:8261–8265. [PubMed: 3141925]
6. Prestera T, Talalay P. Proc Natl Acad Sci U S A 1995;92:8965–8969. [PubMed: 7568053]
7. Zhang DD. Drug Metab Rev 2006;38:769–789. [PubMed: 17145701]
8. Hong F, Sekhar KR, Freeman ML, Liebler DC. J Biol Chem 2005;280:31768–31775. [PubMed: 15985429]
9. Levonen AL, Landar A, Ramachandran A, Ceaser EK, Dickinson DA, Zanoni G, Morrow JD, Darley-Usmar VM. Biochem J 2004;378:373–382. [PubMed: 14616092]
10. Dickinson DA, Levonen AL, Moellering DR, Arnold EK, Zhang H, Darley-Usmar VM, Forman HJ. Free Radic Biol Med 2004;37:1152–1159. [PubMed: 15451055]
11. Gong P, Stewart D, Hu B, Li N, Cook J, Nel A, Alam J. Antioxid Redox Signal 2002;4:249–257. [PubMed: 12006176]
12. Straus DS, Pascual G, Li M, Welch JS, Ricote M, Hsiang CH, Sengchanthalangsy LL, Ghosh G, Glass CK. Proc Natl Acad Sci U S A 2000;97:4844–4849. [PubMed: 10781090]
13. Cernuda-Morollon E, Pineda-Molina E, Canada FJ, Perez-Sala D. J Biol Chem 2001;276:35530–35536. [PubMed: 11466314]
14. Han D, Canali R, Garcia J, Aguilera R, Gallaher TK, Cadenas E. Biochemistry 2005;44:11986–11996. [PubMed: 16142896]

15. Garcia-Pineres AJ, Castro V, Mora G, Schmidt TJ, Strunck E, Pahl HL, Merfort I. J Biol Chem 2001;276:39713–39720. [PubMed: 11500489]
16. Rossi A, Kapahi P, Natoli G, Takahashi T, Chen Y, Karin M, Santoro MG. Nature 2000;403:103–108. [PubMed: 10638762]
17. Musiek ES, Gao L, Milne GL, Han W, Everhart MB, Wang D, Backlund MG, DuBois RN, Zanoni G, Vidari G, Blackwell TS, Morrow JD. J Biol Chem 2005;280:35562–35570. [PubMed: 16100121]
18. Ricote M, Li AC, Willson TM, Kelly CJ, Glass CK. Nature 1998;391:79–82. [PubMed: 9422508]
19. Forman BM, Tontonoz P, Chen J, Brun RP, Spiegelman BM, Evans RM. Cell 1995;83:803–812. [PubMed: 8521497]
20. LoPachin RM, Barber DS. Toxicol Sci 2006;94:240–255. [PubMed: 16880199]
21. Hinman A, Chuang HH, Bautista DM, Julius D. Proc Natl Acad Sci U S A 2006;103:19564–19568. [PubMed: 17164327]
22. Macpherson LJ, Dubin AE, Evans MJ, Marr F, Schultz PG, Cravatt BF, Patapoutian A. Nature 2007;445:541–545. [PubMed: 17237762]
23. d'Ischia M, Rega N, Barone V. Tetrahedron 1999;55:9297–9308.
24. Baker PR, Schopfer FJ, Sweeney S, Freeman BA. Proc Natl Acad Sci U S A 2004;101:11577–11582. [PubMed: 15273286]
25. Schopfer FJ, Lin Y, Baker PR, Cui T, Garcia-Barrio M, Zhang J, Chen K, Chen YE, Freeman BA. Proc Natl Acad Sci U S A 2005;102:2340–2345. [PubMed: 15701701]
26. Cui T, Schopfer FJ, Zhang J, Chen K, Ichikawa T, Baker PR, Batthyany C, Chacko BK, Feng X, Patel RP, Agarwal A, Freeman BA, Chen YE. J Biol Chem 2006;281:35686–35698. [PubMed: 16887803]
27. Baker PR, Lin Y, Schopfer FJ, Woodcock SR, Groeger AL, Batthyany C, Sweeney S, Long MH, Iles KE, Baker LM, Branchaud BP, Chen YE, Freeman BA. J Biol Chem 2005;280:42464–42475. [PubMed: 16227625]
28. Napolitano A, Camera E, Picardo M, d'Ischia M. J Org Chem 2000;65:4853–4860. [PubMed: 10956463]
29. O'Donnell VB, Eiserich JP, Chumley PH, Jablonsky MJ, Krishna NR, Kirk M, Barnes S, Darley-Usmar VM, Freeman BA. Chem Res Toxicol 1999;12:83–92. [PubMed: 9894022]
30. Wright MM, Schopfer FJ, Baker PR, Vidyasagar V, Powell P, Chumley P, Iles KE, Freeman BA, Agarwal A. Proc Natl Acad Sci U S A 2006;103:4299–4304. [PubMed: 16537525]
31. Trostchansky A, Souza JM, Ferreira A, Ferrari M, Blanco F, Trujillo M, Castro D, Cerecetto H, Baker PR, O'Donnell VB, Rubbo H. Biochemistry 2007;46:4645–4653. [PubMed: 17373826]
32. Levy BD, Clish CB, Schmidt B, Gronert K, Serhan CN. Nat Immunol 2001;2:612–619. [PubMed: 11429545]
33. Schwab JM, Serhan CN. Curr Opin Pharmacol 2006;6:414–420. [PubMed: 16750421]
34. Gao L, Wang J, Sekhar KR, Yin H, Yared NF, Schneider SN, Sasi S, Dalton TP, Anderson ME, Chan JY, Morrow JD, Freeman ML. J Biol Chem 2006;282:2529–2537. [PubMed: 17127771]
35. Batthyany C, Schopfer FJ, Baker PRS, Duran R, Baker LMS, Huang Y, Cervenansky C, Branchaud BP, Freeman BA. J Biol Chem 2006;281:20450–20463. [PubMed: 16682416]
36. Anslyn, EV.; Dougherty, DA. Modern Physical Organic Chemistry. University Science Books; Sausalito, CA: 2006.
37. Lowry, TH.; Richardson, KS. Mechanism and Theory in Organic Chemistry. Harper Collins Publishers; New York, NY: 1987.
38. Dickinson DA, Forman HJ. Ann N Y Acad Sci 2002;973:488–504. [PubMed: 12485918]
39. Strange RC, Jones PW, Fryer AA. Toxicol Lett 2000;112–113:357–363.
40. Stamatakis K, Perez-Sala D. Ann N Y Acad Sci 2006;1091:548–570. [PubMed: 17341644]
41. Woodcock SR, Marwitz AJ, Bruno P, Branchaud BP. Org Lett 2006;8:3931–3934. [PubMed: 16928041]
42. Radi R, Beckman JS, Bush KM, Freeman BA. J Biol Chem 1991;266:4244–4250. [PubMed: 1847917]
43. Napolitano A, Crescenzi O, Camera E, Giudicianni I, Picardo M, d'Ischia M. Tetrahedron 2004;58:5061–5067.

44. Alexander RL, Bates DJ, Wright MW, King SB, Morrow CS. Biochemistry 2006;45:7889–7896. [PubMed: 16784241]
45. Doorn JA, Petersen DR. Chem Biol Interact 2003;143–144:93–100.
46. Trujillo M, Radi R. Arch Biochem Biophys 2002;397:91–98. [PubMed: 11747314]
47. Chen Y, Morrow JD, Roberts LJ 2nd. J Biol Chem 1999;274:10863–10868. [PubMed: 10196163]
48. Bogaards JJ, Venekamp JC, van Bladeren PJ. Chem Res Toxicol 1997;10:310–317. [PubMed: 9084911]
49. Song M, Kellum JA, Kaldas H, Fink MP. J Pharmacol Exp Ther 2004;308:307–316. [PubMed: 14569076]
50. Fink MP. Crit Care Med 2003;31:2400–2402. [PubMed: 14501975]
51. Sappington PL, Cruz RJ Jr, Harada T, Yang R, Han Y, Englert JA, Ajami AA, Killeen ME, Delude RL, Fink MP. Biochem Pharmacol 2005;70:1579–1592. [PubMed: 16226725]
52. Pearson RG, Sobel H, Songstad J. J Am Chem Soc 1968;90:319–326.
53. Phan TB, Breugst M, Mayr H. Angew Chem Int Edit 2006;45:3869–3874.
54. Bernasconi CF, Killion RB Jr. J Am Chem Soc 1988;110:7506–7512.
55. Schopfer FJ, Baker PR, Giles G, Chumley P, Batthyany C, Crawford J, Patel RP, Hogg N, Branchaud BP, Lancaster JR Jr, Freeman BA. J Biol Chem 2005;280:19289–19297. [PubMed: 15764811]
56. Gorczynski MJ, Huang J, King SB. Org Lett 2006;8:2305–2308. [PubMed: 16706512]
57. Trujillo M, Budde H, Pineyro MD, Stehr M, Robello C, Flohe L, Radi R. J Biol Chem 2004;279:34175–34182. [PubMed: 15155760]
58. Clavreul N, Adachi T, Pimental DR, Ido Y, Schoneich C, Cohen RA. FASEB J 2006;20:518–520. [PubMed: 16415107]
59. Viner RI, Ferrington DA, Williams TD, Bigelow DJ, Schoneich C. Biochem J 1999;340:657–669. [PubMed: 10359649]
60. Carballal S, Radi R, Kirk MC, Barnes S, Freeman BA, Alvarez B. Biochem 2003;42:9906–9914. [PubMed: 12924939]
61. Lima ES, Di Mascio P, Abdalla DS. J Lipid Res 2003;44:1660–1666. [PubMed: 12837858]

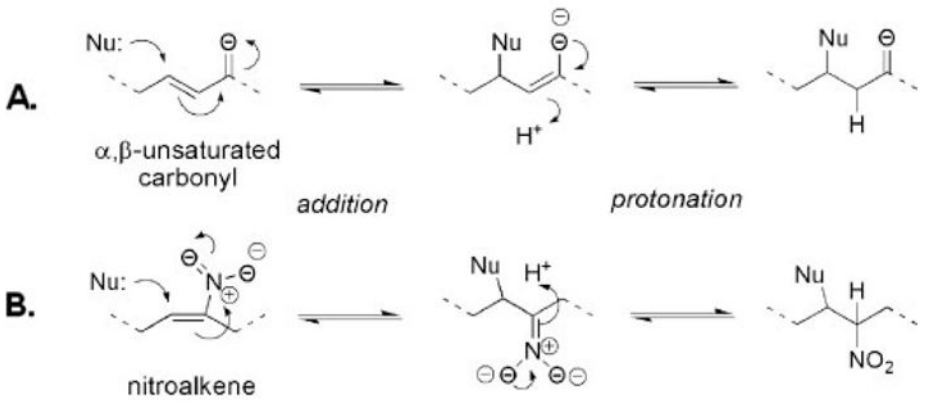


**FIGURE 1. Mechanism of Michael addition reaction**

*A*, reaction of nucleophile (*Nu*) with an *α*,*β*-unsaturated carbonyl enone. The nucleophile reacts at the electrophilic *β*-position to form an adduct. *B*, reaction of nucleophile (such as thiolate) with a conjugated nitroalkene.

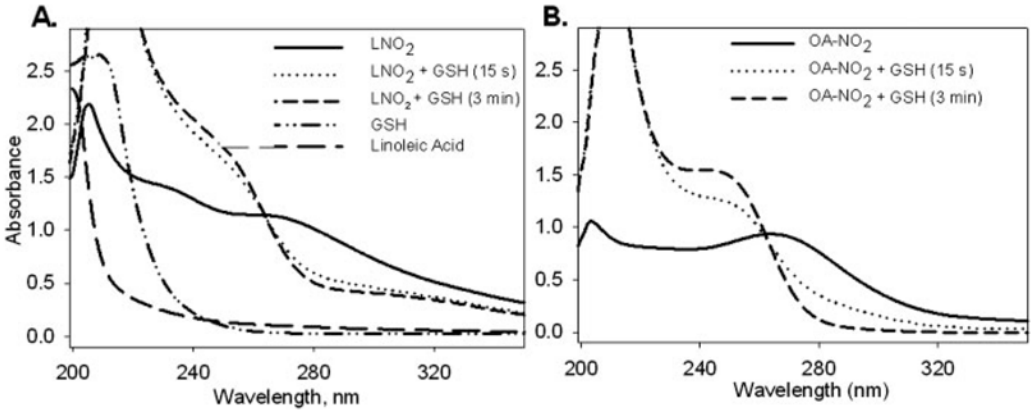


**FIGURE 2. Spectral analysis of nitro-fatty acid reactions with GSH**

Spectral scans of GSH (1 mM) and (*A*) $LNO_2$ (100 $\mu$M) or (*B*) OA-$NO_2$ (100 $\mu$M) were performed in 100 mM potassium phosphate, pH 7.4 using a diode array spectrophotometer between 200 – 400 nm. Free linoleic acid (100 $\mu$M) was also scanned separately for spectral comparisons with $LNO_2$.

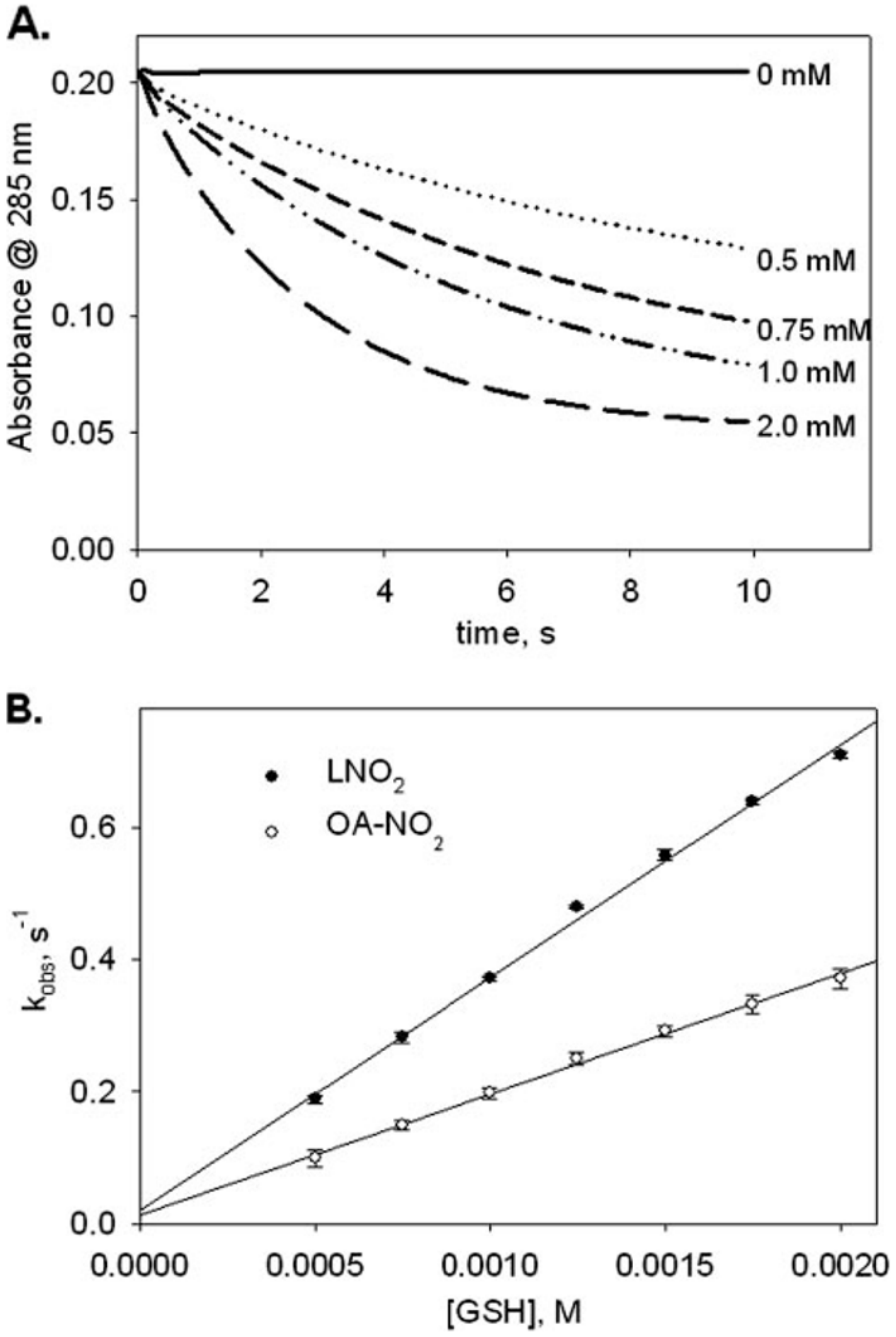


**FIGURE 3. Kinetics of nitro-fatty acid reactions with GSH**

*A*, rate of decrease in OA-$NO_2$ absorbance at 285 nm was monitored on a stopped-flow spectrophotometer. Reactions were started by mixing increasing concentrations of GSH (0–2 mM) with OA-$NO_2$ (0.02 mM), and nitroalkene absorbance decay was monitored at 285 nm. GSH concentration (mM) used for each reaction progression is noted at the end of each run. *B*, apparent pseudo-first-order rate constants ($k_{obs}$) acquired from single exponential curve fits of the reaction progressions were plotted against [GSH]. The slope of the linear regression curve fit is equal to the apparent second-order rate constant, $k_{app}$. Data shown are for experiments with $LNO_2$ (*solid circles*) and OA-$NO_2$ (*unfilled circles*) and are expressed as

mean ± S.D. from three or more separate experiments. The standard deviation bar is not discernible from individual data points in all cases.

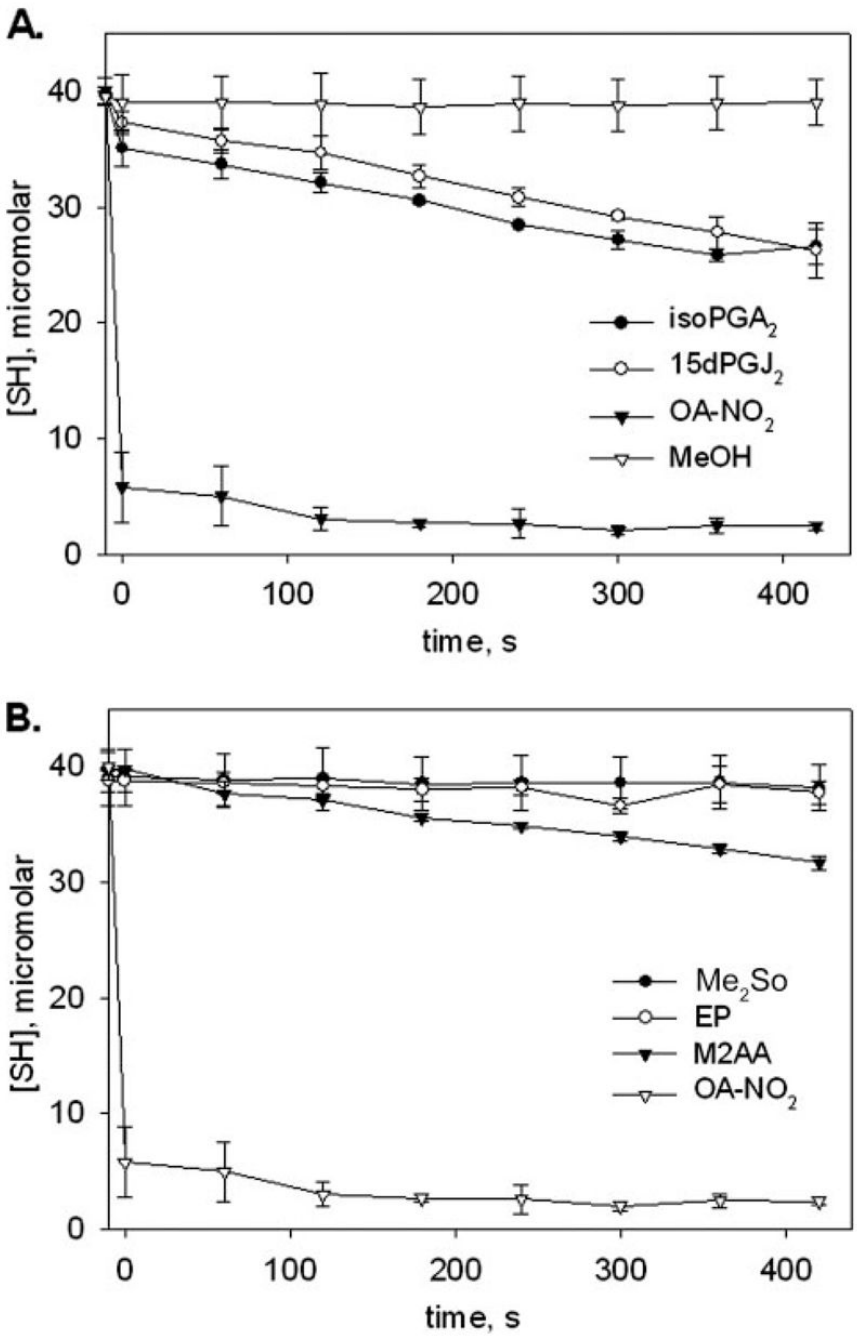


**FIGURE 4. Comparison of reaction rates for prostaglandins and nitro-fatty acids**

*A*, an excess concentration (1.3 mM) of OA-$NO_2$ (*filled squares*), 8-iso-$PGA_2$ (*filled circles*), or 15-deoxy-$\Delta^{12,14}$-$PGJ_2$ (*unfilled triangles*) was reacted against GSH (0.388 mM) at pH 7.4, 37 °C. Aliquots (100 $\mu$l) were removed over time, reactions were stopped with 5× DTNB and then diluted with 50 mM Tris, pH 8.0 prior to thiol quantification at 412 nm. MeOH (40 $\mu$l, *unfilled diamonds*) was added to one reaction as a control, and GSH thiol content was assessed as above. Unaltered $A_{412}$ readings were plotted against time to give a visual representation of reaction rates. Data are expressed as mean ± S.D. for three separate experiments. Calculated apparent second-order rate constants for the prostaglandins appear in Table 2. *B*, above experiment was repeated with the electrophiles ethyl pyruvate (*EP*, *unfilled circles*) and

methyl-2-acetamidoacrylate (*M2AA, filled triangles*), and compared with the vehicle control (*DMSO, filled circles*) and OA-$NO_2$ (*unfilled triangles*).

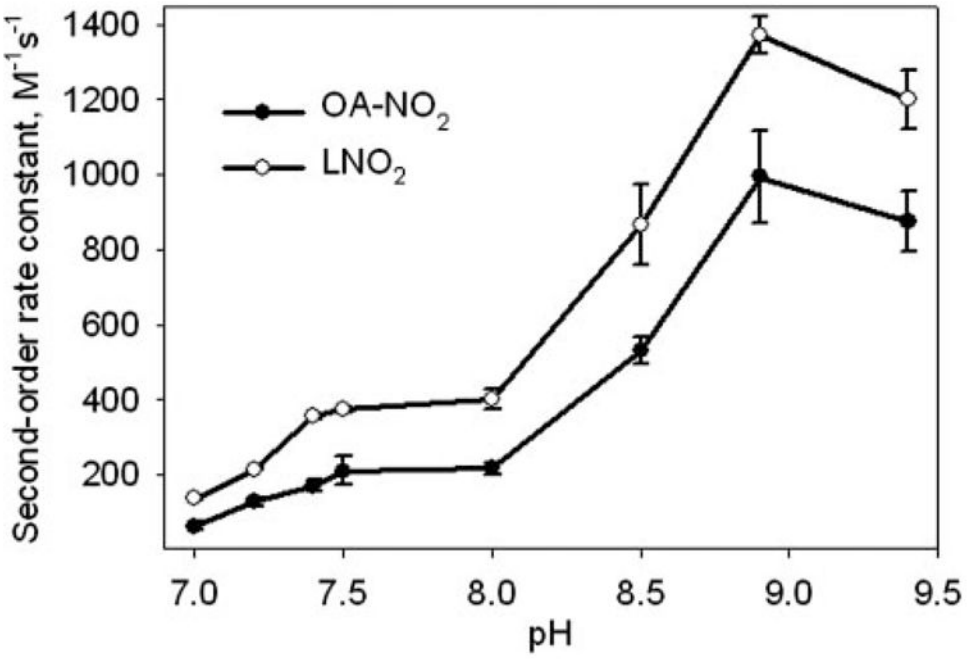


**FIGURE 5. Effect of pH on nitro-fatty acid reaction rates**

Reactions of GSH (0 –2 mM) and OA-$NO_2$ (0.02 mM, *solid circles*) or $LNO_2$ (0.02 mM, *unfilled circles*) were followed by monitoring the decay of nitroalkene absorbance at 285 nm over a range of pH values, as described under "Experimental Procedures." For the pH range 7.0 –7.5, 100 mM potassium phosphate buffers were used, and for the pH range 8.0 –9.4, 100 mM Tris buffers were used. Second-order rate constants were plotted for a range of pH values. Data are expressed as mean ± S.D. from three or more separate experiments.

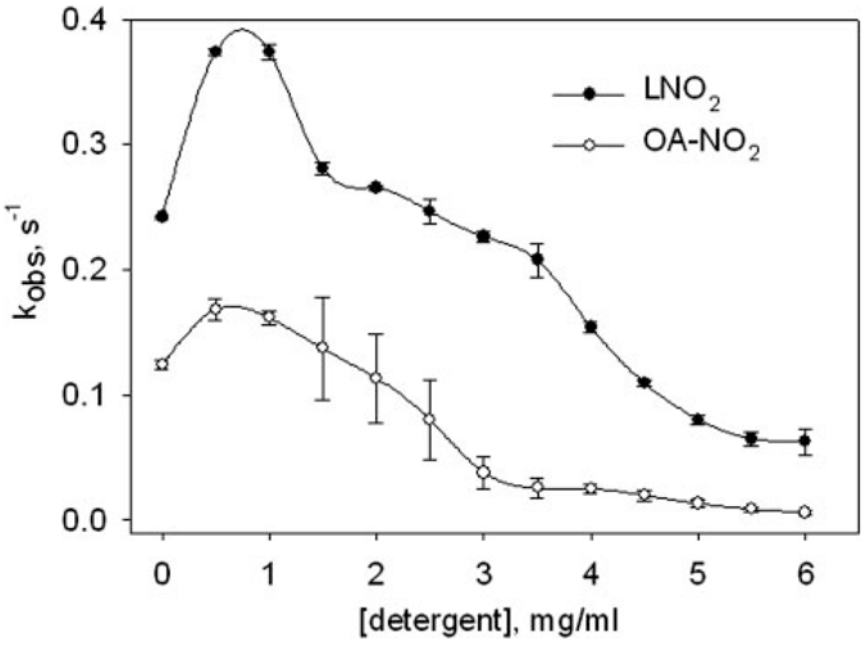


**FIGURE 6. Kinetic analysis of micellar inhibition of nitro-fatty acid reactions with GSH**

$OA\text{-}NO_2$ (*unfilled circles*, 0.02 mM) or $LNO_2$ (*filled circles*, 0.02 mM) were reacted with GSH (1 mM) on the stopped flow spectrophotometer as described under "Experimental Procedures," except the reaction buffer contained 0 – 6 mg/ml of octyl-*β*-D-glucopyranoside. The obtained pseudo-first-order reaction rate was plotted against detergent concentration. Data are expressed as mean ± S.D. from three or more separate experiments.

## TABLE 1

**Second-order rate constants for nitro-fatty acid reaction with thiols**

Rates for GSH (0–2.0 mM) and nitroalkene (0.02 mM) reactions were obtained as described under "Experimental Procedures" at pH 7.4 and 37 °C. All data are expressed as mean ± S.D. $LNO_2$ and OA-$NO_2$ preparations were mixed regio-isomers.

| Nitroalkene | GSH | Cys |
|---|---|---|
| | | $M^{-1}s^{-1}$ |
| OA-$NO_2$ | 183 ± 6 | 267 ± 33 |
| $C^9$-OA-$NO_2$ | 174 ± 7 | 287 ± 14 |
| $LNO_2$ | 355 ± 5[a] | 522 ± 36[a] |

[a] Represents significantly different from OA-$NO_2$, as determined using a two-tailed, unpaired Student's *t* test, with a $p < 0.05$.

## TABLE 2

**Second-order rate constants for oxidant and electrophilic lipid reaction with thiols**

Rate constants were determined at pH 7.4, 37 °C; however, the range of [GSH] used for analysis and the concentration of oxidant, electrophilic lipid may vary for cited rate constants. Data are expressed as mean ± S.D.

| Oxidant/electrophilic lipid | Second-order rate constant | Ref. |
|---|---|---|
| | $M^{-1}s^{-1}$ | |
| $ONOO^-$ | 1350 | 46 |
| $H_2O_2$ | 2.6 ± 0.9 | This work |
| 4-Hydroxynonenal | 1.3 | 45 |
| 4-Oxononenal | 145 | 45 |
| 8-*iso* Prostaglandin $A_2$ | 0.7 ± 0.2 | This work |
| 15-*deoxy*-$\Delta^{12,14}$-Prostaglandin $J_2$ | 0.7 ± 0.3 | This work |
| OA-$NO_2$ | 183 ± 6 | This work |
| $LNO_2$ | 355 ± 5 | This work |

**TABLE 3**

Second-order rate constants for OA-$NO_2$ reaction with thiols of different p$K_a$

| Thiol | p$K_a$[a] | $k_{app}$ |
|---|---|---|
| | | $M^{-1}s^{-1}$ |
| Cysteine methyl ester | 6.7 | 442 ± 9 |
| Penicillamine | 7.9 | 71 ± 5 |
| Cysteine | 8.3 | 267 ± 33 |
| Glutathione | 8.8 | 183 ± 6 |
| Homocysteine | 8.9 | 100 ± 2 |
| *N*-Acetyl-cysteine | 9.5 | 28 ± 3 |
| Dihydrolipoic acid[b] | 10.7 | 13 ± 3 |

[a] Data for thiol p$K_a$ were obtained from Ref. 46.

[b] Calculated assuming both thiols are equally reactive with OA-$NO_2$.